Journal of Molecular Catalysis A: Chemical 319 (2010) 52–57

Contents lists available at ScienceDirect

Journal of Molecular Catalysis A: Chemical

journal homepage: www.elsevier.com/locate/molcata

Structural characterization and dehydration activity of CeO_2–SiO_2 and CeO_2–ZrO_2 mixed oxides prepared by a rapid microwave-assisted combustion synthesis method

Benjaram M. Reddy*, Gunugunuri K. Reddy, Lakshmi Katta

Inorganic and Physical Chemistry Division, Indian Institute of Chemical Technology, Uppal Road, Tarnaka, Hyderabad, AP 500607, India

ARTICLE INFO

Article history:
Received 9 July 2009
Received in revised form
19 November 2009
Accepted 29 November 2009
Available online 4 December 2009

Keywords:
Dehydration
4-Methylpentan-2-ol
Microwave dielectric heating
Solution combustion synthesis
CeO_2
Acid–base properties
Catalyst characterization

ABSTRACT

Catalytic performance of ceria–silica and ceria–zirconia mixed oxides for dehydration of 4-methylpentan-2-ol has been investigated. The reaction was carried out in the temperature region 523–673 K in a fixed-bed microreactor at normal atmospheric pressure. The investigated mixed oxides were prepared by a rapid microwave-assisted combustion synthesis method by using metal nitrates as precursors. X-ray diffraction (XRD), Raman spectroscopy (RS) and temperature programmed desorption (TPD) techniques were used to investigate the structural and surface properties of the mixed oxides. XRD studies revealed the formation of a specific $Ce_{0.5}Zr_{0.5}O_2$ solid solution in case of ceria–zirconia sample, and the ceria–silica mixed oxide is found to be in amorphous form. RS measurements suggest the presence of oxygen vacancies and lattice defects in the ceria–zirconia mixed oxide sample. TPD of ammonia and CO_2 results reveal that ceria–silica exhibits strong acid–base properties compared to ceria–zirconia mixed oxide. Good alcohol conversion and excellent 4-methylpent-1-ene selectivity were observed on both the mixed oxides.

1. Introduction

Since the pioneering work of Pines and Pillai [1] on alumina, the dehydration of secondary alcohols over metal oxides has been widely investigated [2,3]. Thoria and other actinide or lanthanide oxides have been reported to be selective towards alk-1-ene formation [4–6]. Ceria-based catalysts are known to exhibit a high selectivity towards the formation of 1-alkenes in the dehydration of secondary alcohols [7]. A useful application seems to be the dehydration of 4-methylpentan-2-ol, which could represent an alternative route to the preparation of 4-methylpent-1-ene, an intermediate for manufacturing thermoplastic polymers of high technological significance. Besides the desired 1-alkene, the alcohol dehydration always leads to the formation of 4-methylpent-2-ene, often accompanied by skeletal isomers of C_6-alkenes [8]. In addition, dehydrogenation to 4-methylpentan-2-one can occur simultaneously with dehydration [8]. Pure ceria did not exhibit good catalytic behaviour leading preferentially to 2-alkenes, while a high selectivity to 1-alkene could be reached by doped ceria-based materials [9]. Previous results on several oxide [10,11] and zeolite catalysts [12] showed that the high selectivity to 1-alkene requires fine-tuning of the acid–base properties of the catalyst, in order to avoid dehydration to the undesired 2-alkene, as well as parasitic formation of ketone through the competing dehydrogenation pathway. As known from literature, doped ceria-based materials exhibit better acid–base properties compared to pure ceria [7]. Recent results reveal that zirconia and silica containing ceria-based materials exhibit good activity for dehydration reactions [9,13].

It was noticed that the CeO_2–ZrO_2 catalysts exhibit good catalytic activity and the acid–base character of the catalyst is most important in order to obtain high selectivity to the desired 1-alkene and to avoid the formation of olefins with internal double bonds and the dehydrogenation product ketone [11]. It is a well-known fact in the literature that synthesis methodology and process conditions strongly influence the acid–base properties of the mixed oxides [14,15]. So far various methods have been employed to prepare ceria-based mixed oxides, which include precipitation [16], precursor modification [17], sol–gel [18], surfactant-assisted [19], micro-emulsion [20], hydrothermal–solvothermal [21], spray pyrolysis [22], sputtering [23], chemical vapor deposition [24] and supercritical water synthesis [25]. It is well established that preparation methods like coprecipitation can lead to high specific surface area materials; however, the temperature stability of these oxides is characterized by severe loss of surface area at elevated temperatures. Further, the wet chemical routes require calcination at high

* Corresponding author. Tel.: +91 40 27191714; fax: +91 40 27160921.
E-mail addresses: bmreddy@iict.res.in, mreddyb@yahoo.com (B.M. Reddy).

1381-1169/$ – see front matter © 2009 Elsevier B.V. All rights reserved.
doi:10.1016/j.molcata.2009.11.020

temperatures for prolonged times which lead to crystallite growth and decrease in the reactivity. Synthetic methodologies based on sol–gel and related routes require expensive precursors, such as alkoxides. Among the various solution routes employed, the solution combustion process is simple, fast, yields high surface area products of desired composition [26]. The solution combustion process is an attractive synthetic route particularly for the preparation of multicomponent oxide materials, since the homogeneity of the aqueous solution of the salts is preserved in the combustion residue [27]. In addition to better homogeneity and purity of the products, the solution combustion method has the advantage of doping desired amounts of impurity ions and a low processing temperature leading to uniform crystalline particle size at superfine dimensions [28].

In the present paper we report on the synthesis of CeO_2–SiO_2 (MWCS) and CeO_2–ZrO_2 (MWCZ) mixed oxides by a solution combustion synthesis method using microwave dielectric heating. The resultant catalysts were characterized by BET surface area, XRD, Raman, TPD of NH_3 and CO_2 techniques, and evaluated for dehydration of 4-methylpentan-2-ol.

2. Experimental

2.1. Catalyst preparation

Ceria–silica and ceria–zirconia mixed oxides (1:1 mole ratio based on oxides) were prepared by a simple and rapid microwave-assisted solution combustion synthesis method. Metal nitrates namely, $Ce(NO_3)_3$, $SiO(NO_3)_2$ and $ZrO(NO_3)_2$ were used as precursors since nitrates favor combustion. To prepare ceria–silica mixed oxide, the requisite quantities of cerium(III) nitrate (Aldrich, AR grade) and silica(IV) oxinitrate (Fluka, AR grade) were dissolved separately in deionized water and mixed together in a Pyrex glass dish. A stoichiometric quantity (as per the concept used in propellant chemistry) of solid urea (Fluka, AR grade) was added to the aforementioned mixture solution and stirred rigorously to obtain a clear solution. The dish containing the reaction mixture was introduced into a modified domestic microwave oven having an exhaust opening at the top of the oven and working at atmospheric pressure (BPL, India Limited, BMO-700T, 2.54 GHz, 700 W). Initially, the solution boils and undergoes dehydration followed by decomposition and spontaneous combustion with the evolution of large amounts of gases, including N_2, CO_2 and H_2O along with some small traces of NH_3 and NO_2, followed by a rapid flame resulting in a light yellow residual mass. The entire process in the microwave oven from dehydration to combustion took around 40 min. Three to four experiments were conducted under identical conditions to check for reproducibility. Properties of all the synthesized powders were found to be identical. Ceria–zirconia mixed oxide was also prepared in the same way.

2.2. Catalyst characterization

The BET surface areas of the powders were determined by N_2 adsorption at liquid nitrogen temperature using a Micromeritics Gemini 2360 instrument. Prior to analysis, samples were oven dried at 393 K for 12 h and flushed with Argon gas for 2 h. XRD patterns were recorded on a Bruker (Karlsruhe, Germany) D8 advanced system using a diffracted beam monochromated Cu Kα (0.15418 nm) radiation source. The intensity data were collected over a 2θ range of 3–80° with a 0.02° step size and using a counting time of 1 s per point. Crystalline phases were identified by comparison with the reference data from the International Centre for Diffraction Data (ICDD). The average crystallite size of the oxide phases was estimated employing Scherrer equation and considering the XRD data of all prominent lines [29]. The Raman spectra were recorded on a triple subtractive Jobin Yvon T64000 Raman spectrometer equipped with a liquid nitrogen-cooled charge-coupled device (CCD) detector. The emission line at 514.5 nm from the Ar^+ Ion laser was focused on the sample under the microscope, with the width of the analyzed spot being about 1 μm. The power of the incident beam on the sample was about 5 mW. The TPD measurements were performed on a Micromeritics AutoChem 2910 instrument. A thermal conductivity detector was used for continuous monitoring of the desorbed ammonia and the areas under the peaks were integrated. Prior to TPD measurements, samples were pretreated at 573 K for 1 h, after pretreatment the samples were saturated with 4% ultra-pure anhydrous ammonia for 1 h and subsequently flushed with He to remove the physisorbed ammonia.

2.3. Dehydration activity

Dehydration activity measurements were carried out in a down flow fixed-bed microreactor heated by means of a tubular furnace in a previously described apparatus [30,31]. The reactor–catalyst load consisted of 0.5 g of catalyst diluted with quartz fractions. The catalyst was treated using CO_2-free airflow at 673 K for 5 h, prior to the reaction. The 4-methylpentan-2-ol was fed with N_2 stream, into the vaporizer at a flow rate of 1.5 ml/h. The flow rate of dry N_2 was maintained at 60–70 ml min^{-1}. The reaction was carried out in the temperature region 523–673 K. The liquid products were collected in ice cold freezing traps and were analyzed by a gas chromatograph with flame ionization detector (FID). The activity data was collected under steady state conditions. The conversions and product selectivity were calculated as per the procedure described elsewhere [32].

3. Results and discussion

The X-ray powder diffraction patterns of the two mixed oxides prepared in the present study are shown in Fig. 1. As can be noted from this figure, the ceria–silica mixed oxide exhibits amorphous nature. It is difficult to resolve the peaks. Formation of solid solution of specific composition $Ce_{0.5}Zr_{0.5}O_2$ (PDF-ICDD 34-1436) has been conferred in the case of ceria–zirconia mixed oxide. This is pri-

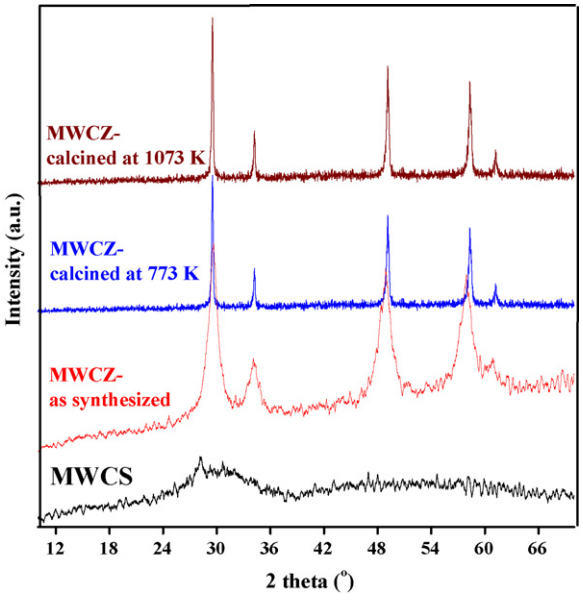

Fig. 1. X-ray powder diffraction patterns of ceria–silica and ceria–zirconia mixed oxides (MWCS: ceria–silica, MWCZ: ceria–zirconia).

Table 1
BET surface area, crystallite size, and total amount of NH_3 and CO_2 desorbed pertaining to ceria–silica and ceria–zirconia mixed oxides (MWCS: ceria–silica, MWCZ: ceria–zirconia).

Sample	BET surface area (m^2/g)	Crystallite size (nm)	Total NH_3 desorbed (μ mole/m^2)	Total CO_2 desorbed (μ mole/m^2)
MWCS	125	n.d.	3.82	5.08
MWCZ	56	12.5	2.31	3.20

n.d.: not determined.

marily due to incorporation of Zr^{4+} cations into the cubic fluorite structure of ceria as reported by several authors [33,34]. To confirm its presence, the synthesized sample was again subjected to thermal treatments at 773 and 1073 K. An increase in the intensity of lines due to better crystallization of the phase was noted as shown in Fig. 1. No big change was noted in the case of ceria–silica sample. There is no evidence for the formation of t-ZrO_2 or m-ZrO_2 phases of zirconia within the detection limits of the XRD technique. As known from the literature, substitution of some of the Ce^{4+} ions by Zr^{4+} favors the formation of defects in the ceria–zirconia lattice that induces a distortion of the oxygen sublattice. If the ceria–zirconia solid solution contains less zirconium, it cannot induce sufficient stress and the oxygen mobility within the bulk. On the other hand if the zirconium content is too high (more than 50%) it will reduce the quantity of the redox element Ce [35]. Therefore, for an intermediate composition range i.e. $Ce_{0.5}Zr_{0.5}O_2$ there is an optimum balance between amount of redox elements and number of defects and consequently the oxygen storage capacity (OSC) of the mixed oxide is maximum. Formation of $Ce_{0.5}Zr_{0.5}O_2$ solid solution is an interesting observation from the present study. However, in our previous reports formation of $Ce_{0.75}Zr_{0.25}O_2$ solid solution was observed for ceria–zirconia mixed oxides prepared by conventional coprecipitation method with the same presently used composition [33]. Crystallite sizes of CeO_2 in CeO_2–SiO_2, and $Ce_{0.5}Zr_{0.5}O_2$ in CeO_2–ZrO_2 are summarized in Table 1. As can be noted from Table 1, the crystallite size depends on the type of foreign oxide present. In general, as expected the crystallite size of ceria in ceria–silica mixed oxide is relatively small compared to ceria–zirconia. This may be due to stabilization of smaller ceria particles over the surface of silica. The N_2 BET surface values of two mixed oxides prepared in the present study are presented in Table 1. Both the mixed oxides exhibit relatively high specific surface areas. As expected ceria–silica mixed oxide (125 m^2/g) exhibits more specific surface area than ceria–zirconia mixed oxide (56 m^2/g).

To understand thermal stability and phase segregation, the as synthesized ceria–zirconia mixed oxide sample was subjected to thermal treatment at two different temperatures (773 and 1073 K). The X-ray powder diffraction patterns of as synthesized ceria–zirconia and calcined ceria–zirconia at two different temperatures are represented in Fig. 1. The crystallinity was increased as we go from as synthesized sample to 773 K and increased further after calcination at 1073 K. The increase in the crystallite size is due to better crystallization during prolonged heating. During the preparation of the mixed oxide the precursor solution was exposed to microwaves for 40 min. But additional calcination was done by using conventional heating source for 6 h. Formation of a monophasic solid solution of composition $Ce_{0.5}Zr_{0.5}O_2$ has been clearly established. Interestingly, no phase segregation phenomenon was observed with increasing treatment temperature in the present study. However, in our previous studies, an unambiguous phase segregation phenomenon was noted with increasing calcination temperature from 773 to 1073 K for the same samples prepared by conventional coprecipitation method [33]. As known from literature, phase segregation leads to decrease in the activity as well as stability [36].

Raman spectra of the two samples prepared in the present study are shown in Fig. 2. As presented in Fig. 2, the Raman spectrum of ceria–silica shows a prominent peak at 464 cm^{-1}. The Raman band at 464 cm^{-1} corresponds to the triply degenerate F_{2g} mode and can be viewed as a symmetric breathing mode of the oxygen atoms around the cerium ions [37]. As reported in the literature, silica did not show any Raman features [38]. In case of ceria–zirconia, the band due to F_{2g} mode has been observed at 474 cm^{-1}. The slight shift in the Raman frequency to higher wave numbers could be due to the incorporation of zirconium ions into the ceria lattice, as evidenced by XRD results. No Raman lines due to ZrO_2 could be observed, which is consistent with XRD measurements. According to literature, six Raman active modes ($A_{1g} + 3E_g + 2B_{1g}$) are expected for t-ZrO_2 (space group *P*42/*nmc*), whereas, for the cubic fluorite structure of CeO_2 (space group *Fm*3*m*), only one mode is Raman active. Along with the intense peak at around 465 cm^{-1}, weak and broad bands at 600 and 620 cm^{-1} are noticed for ceria–silica and ceria–zirconia samples, respectively. These bands correspond to a non-degenerate LO mode of CeO_2 [38,39]. Normally, this mode should not be observed by Raman spectroscopy but the presence of some defects can involve relaxation of selection rules. In particular, this band has been linked to oxygen vacancies in the CeO_2 lattice [39]. In addition to these two bands ceria–zirconia exhibited another band at 300 cm^{-1}. This band is due to the displacement of oxygen atoms from their ideal fluorite lattice positions [40].

Acid–base properties of the synthesized mixed oxides were determined by conducting temperature programmed desorption of CO_2 and ammonia experiments. In general, TPD measurements provide meaningful information about the available adsorption sites as well as the way in which the key species are chemisorbed on the

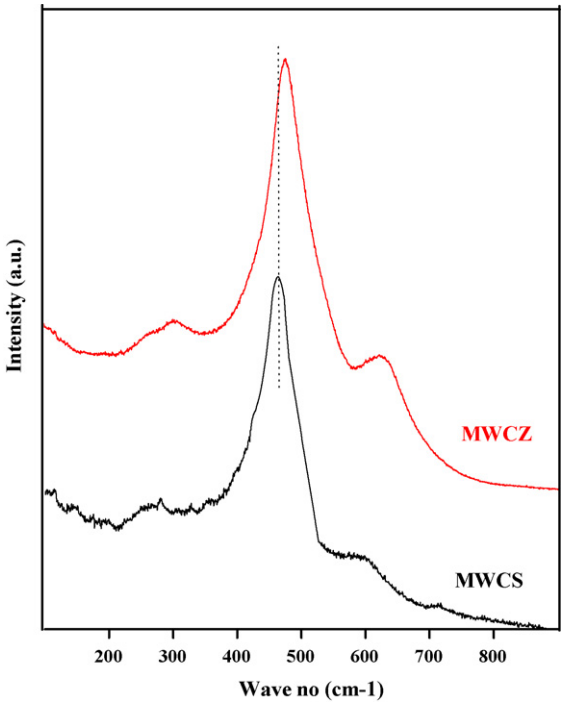

Fig. 2. Raman spectra of ceria–silica and ceria–zirconia mixed oxides (MWCS: ceria–silica, MWCZ: ceria–zirconia).

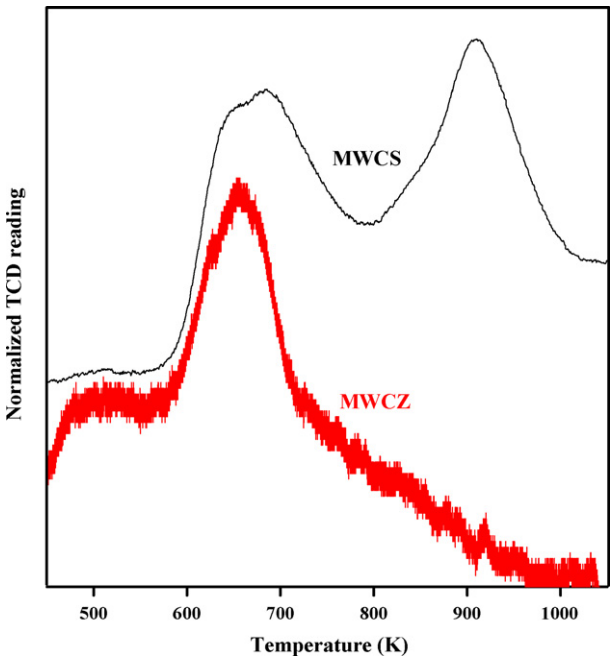

Fig. 3. NH_3 TPD profiles of ceria–silica and ceria–zirconia mixed oxides (MWCS: ceria–silica, MWCZ: ceria–zirconia).

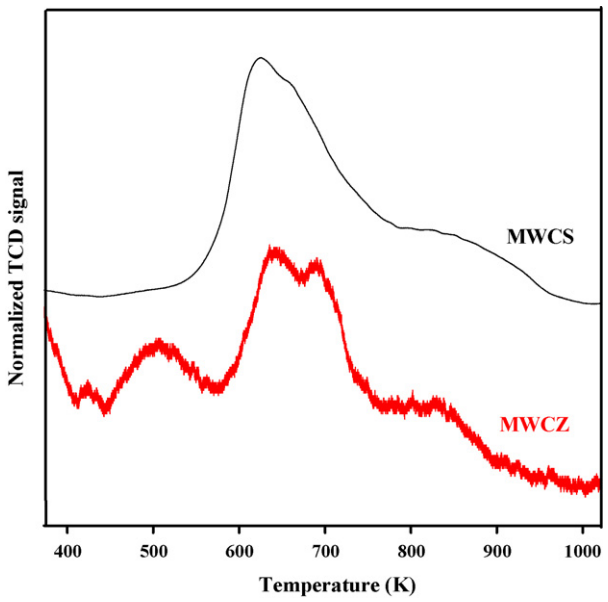

Fig. 4. CO_2 TPD profiles of ceria–silica and ceria–zirconia mixed oxides (MWCS: ceria–silica, MWCZ: ceria–zirconia).

catalyst surface. It is a well known fact in the literature that the selectivity of a product in the dehydration reaction depends on the acid–base properties of the catalysts [30]. NH_3 TPD profiles of both the mixed oxides are shown in Fig. 3. As shown in Fig. 3, ceria–silica mixed oxide exhibits two narrow desorption maxima at around 693 and 899 K. The peak at 693 K represents the acidic sites of medium strength and the narrow peak at 899 K corresponds to NH_3 released from strong acidic sites corresponding to strongest Lewis acid sites present on the catalyst surface. Ceria–zirconia mixed oxide exhibits a broad peak at 462 K and a narrow peak at 625 K. The broad peak at lower temperature corresponds to weak acid sites and the narrow peak at higher temperature is due to strong Lewis acid sites. The amount of NH_3 desorbed is always high for the sample that has high surface area and it is not possible to compare the acidity of the samples by calculating the total amount of ammonia desorbed for each sample. So in the present study the amount of ammonia desorbed per m^2 of surface area was used to compare the acidity of the mixed oxides and the values are presented in Table 1. As shown in Table 1 and Fig. 3, the MWCS sample exhibits more acidity compared to MWCZ sample. More acidity for silica sample might be due to stabilization of nanosized ceria particles over the surface of silica. Fig. 4 represents the CO_2 TPD profiles of both the mixed oxides prepared in the present study. A relatively narrow CO_2 desorption peak at 673 K is observed for the ceria–silica mixed oxide. On the other hand ceria–zirconia mixed oxide exhibits broad desorption peaks. The amount of CO_2 desorbed per m^2 of surface area is given in Table 1. Here too silica sample exhibits more basicity compared to zirconia sample and it can be explained as due to high surface area as well as stabilization of the ceria particles over the silica surface. Interestingly, the amount of CO_2 desorbed is more for both the mixed oxides compared to the amount of NH_3 desorbed. On the whole, more balanced acid–base sites are generated when ceria is dispersed over the surface of silica.

The dehydration of 4-methylpentan-2-ol may lead to different products and the composition of the product mixture depends on the mechanistic pathway of the reaction over the catalyst surface. This involves three types of mechanisms viz., concerted elimination pathway (E2), formation of carbocation (E1) and carbanion formation via two-point mechanism (E1cB) [8,41]. These mechanisms should be regarded as limiting cases, since intermediate situations can occur. Conversion of 4-methylpentan-2-ol has been carried out as a function of temperature and the results are displayed in Fig. 5. No significant changes in the conversion were observed in the runs where both the flow rate and the catalyst amount were significantly changed while keeping the same W/F value; accordingly, the occurrence of external diffusion limitations was ruled out. In general, an increase in the conversion with an increase of temperature was observed. Activity of pure ceria is negligible when compared to silica- and zirconia-based mixed oxides, hence these results are not included in the figures. A nominal conversion of 10% was observed over ceria–zirconia at 523 K, the lowest reaction temperature studied, which increased to 20% at 673 K. On the other hand ceria–silica exhibited a conversion of 25% at 523 K, which increased to 43% at 673 K. The increase in the conversion in case of ceria–silica may be due to better balance of both acid–base properties as well as high surface area. After dispersing ceria over silica, a more balanced

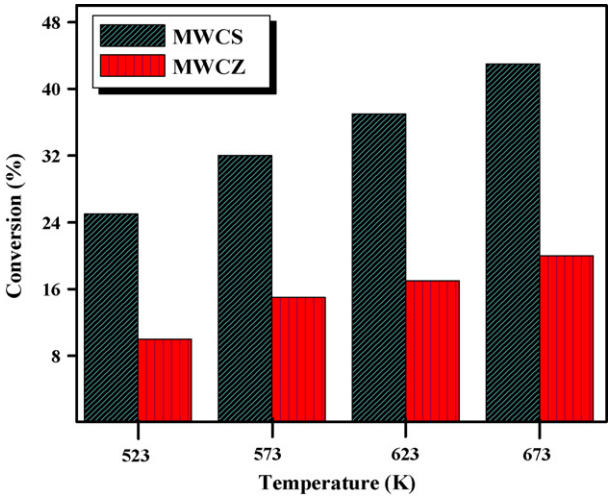

Fig. 5. Alcohol conversion versus temperature dependence curves of ceria–silica and ceria–zirconia mixed oxides for dehydration of 4-methylpentan-2-ol (MWCS: ceria–silica, MWCZ: ceria–zirconia, WHSV: 1.5 ml/h).

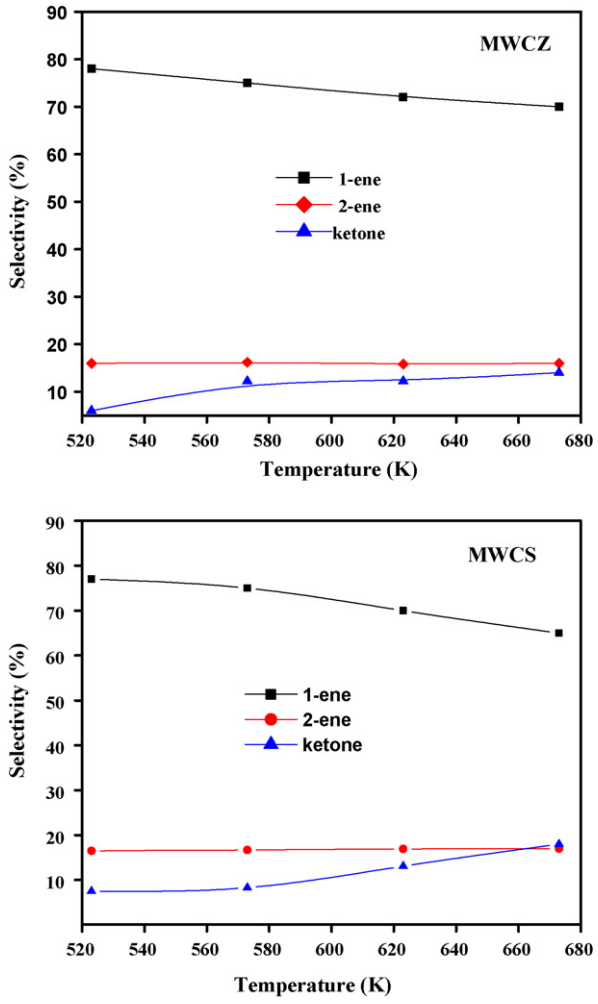

Fig. 6. Product selectivity versus temperature dependence curves of ceria–silica and ceria–zirconia mixed oxides for the dehydration of 4-methylpentan-2-ol (MWCS: ceria–silica, MWCZ: ceria–zirconia, WHSV: 1.5 ml/h).

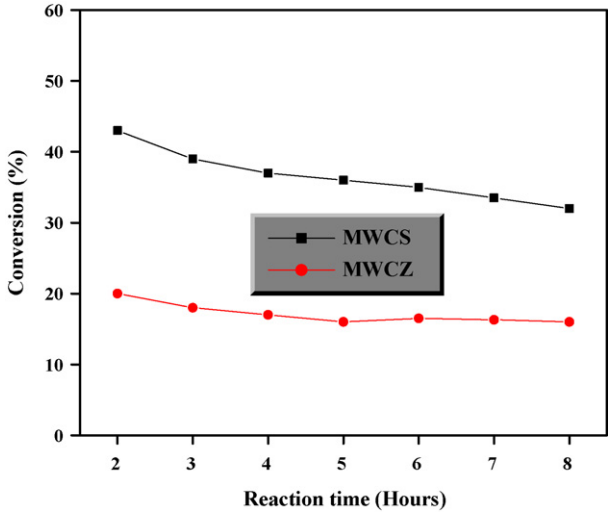

Fig. 7. Alcohol conversion versus time-on-stream dependence curves of ceria–silica and ceria–zirconia mixed oxides for the dehydration of 4-methylpentan-2-ol (MWCS: ceria–silica, MWCZ: ceria–zirconia, WHSV: 1.5 ml/h).

acid–base surface sites could be generated which result in a large increase of conversion.

As regard to selectivities, it can be noted that two catalysts tend to favor the formation of the desired 1-alkene, which is the most abundant product, together with some amounts of 2-alkene and ketone (Fig. 6). As can be observed from Fig. 6, the selectivity of the desired product, 1-alkene decreases with increase of reaction temperature on both the catalysts. On the other hand, the selectivity of the dehydrogenation product, 4-methylpentan-2-one increases with increasing reaction temperature leading to a decrease in the selectivity of the desired product. However, there is no appreciable change in the selectivity of 4-methylpent-2-ene with increasing reaction temperature. If the mechanism of reaction is considered, the first step of alcohol transformation on metal oxide catalysts is the adsorption of the reactant on the surface. The selectivity of secondary alcohol dehydration depends on the competition among the above specified mechanisms: when the acid and base functions of the catalyst are well balanced in terms of site concentrations, a two-point adsorption of the reactant alcohol occurs, in which the most acidic hydrogen (i.e., H of terminal methyl group) interacts with a base site while the acid centre interacts with the OH group of the alcohol. In this situation, the transformation of the adsorbed species into olefin takes place via concerted mechanism (E2 pathway) and 2-alkene is then the preferred product (Saytzeff product). If the acid sites are weak and the base sites are strong enough, rupture of the C–H bond with carbanion formation occurs first and an E1cB mechanism sets in leading to the preferential formation of 1-alkene (Hofmann product). If the acid sites are predominant, the reaction is initiated by the attack of the acid sites to the hydroxy group of the alcohol leading to the formation of a carbocation intermediate, which transforms into alkenes with internal double bonds (E1 mechanism, Saytzeff product). The acid–base properties of the surface govern the competition among the mechanisms, by determining the adsorption mode of the reactant alcohol and the timing of bond rupture [42]. An E1cB mechanism has been proposed for secondary alcohol dehydration on ceria-based mixed oxides in the present study. Both the ammonia and CO_2 TPD results indicate that basic sites are dominating in the mixed oxides compared to the acidic sites. This has previously been shown for the dehydration of 4-methylpentan-2-ol over zirconia, as well as on ceria and lanthana catalysts prepared through the traditional wet inorganic routes [43,44]. Recently, it has also been confirmed over ceria–zirconia solid solutions prepared by ball-milling [11]. The present results are well corroborating with the literature reports. Slightly more selectivity towards 1-ene in case of ceria–zirconia mixed oxide compared to ceria–silica may be due to lower conversion levels. As presented in Fig. 7, both the composite oxide catalysts show some initial deactivation in the time-on-stream experiments, afterwards they exhibit quite stable activity without deactivation. Imbalance of carbon may be the reason for initial deactivation. Recent literature reveals that ceria-based mixed oxides are highly coke resistant and exhibit promising stable activity without deactivation during time-on-stream runs in various reactions [34,45–47]. This was mainly attributed to the availability of lattice oxygen due to oxygen storage and release property of the ceria-based mixed oxides [11,34].

4. Conclusions

Ceria–silica and ceria–zirconia mixed oxides were prepared by a simple and rapid single step microwave-assisted combustion synthesis method with sufficiently high specific surface area. X-ray diffraction results revealed that the CeO_2–SiO_2 mixed oxide exhibits amorphous nature, and a cubic fluorite type solid solution $Ce_{0.5}Zr_{0.5}O_2$ was formed in case of CeO_2–ZrO_2 sample. Raman spectroscopic measurements conclude the presence of lattice defects, oxygen vacancies and displacement of oxygen ions from their ideal lattice positions in CeO_2–ZrO_2 mixed oxide. TPD of NH_3 and CO_2 results suggest that the silica-based mixed oxide exhibits more

acidity as well as basicity compared to the zirconia-based mixed oxide. Both the mixed oxides provided excellent selectivity towards 1-ene. Among the two catalysts investigated, the MWCS sample exhibited better conversion.

Acknowledgements

GKR and LK thank UGC and CSIR, respectively, for a senior research fellowship. Authors thank Dr. I. Ganesh, Senior Scientist, ARCI, Hyderabad for providing some of the results.

References

[1] H. Pines, C.N. Pillai, J. Am. Chem. Soc. 82 (1960) 2401.
[2] H. Pines, J. Manassen, Adv. Catal. 16 (1966) 49.
[3] J.M. Winterbottom, Catalysis 4 (1981) 141.
[4] A.J. Lundeen, R. Van Hoozer, J. Am. Chem. Soc. 85 (1963) 2180.
[5] A.J. Lundeen, R. Van Hoozer, J. Org. Chem. 32 (1967) 3386.
[6] K. Thomke, in: G.C. Bond, P.B. Wells, F.C. Thomkins (Eds.), Proc. Sixth Int. Congr. Catal., vol. 1, The Chemical Society, London, 1977, p. 105.
[7] A. Auroux, P. Artizzu, I. Ferino, R. Monaci, E. Rombi, V. Solinas, G. Petrini, J. Chem. Soc., Faraday Trans. 92 (1996) 2619.
[8] M.G. Cutrufello, I. Ferino, R. Monaci, E. Rombi, V. Solinas, Top. Catal. 19 (2002) 225.
[9] B.M. Reddy, G. Thrimurthulu, P. Bharali, P. Saikia, J. Mol. Catal. A: Chem. 275 (2007) 166.
[10] A. Auroux, P. Artizzu, I. Ferino, V. Solinas, G. Leofanti, M. Padovan, G. Messina, R. Mansani, J. Chem. Soc., Faraday Trans. 91 (1995) 3263.
[11] M.G. Cutrufello, I. Ferino, V. Solinas, A. Primavera, A. Trovarelli, A. Auroux, C. Picciau, Phys. Chem. Chem. Phys. 1 (1999) 3369.
[12] A. Auroux, P. Artizzu, I. Ferino, R. Monaci, E. Rombi, V. Solinas, Micropor. Mater. 11 (1997) 117.
[13] B.M. Reddy, P. Lakshamanan, P. Bharali, P. Saikia, J. Mol. Catal. A: Chem. 258 (2006) 355.
[14] C. de Leitenburg, A. Trovarelli, F. Zamar, S. Maschio, G. Dolcetti, J. Llorca, J. Chem. Soc. Chem. Commun. (1995) 2181.
[15] A. Trovarelli, F. Zamar, J. Llorca, C. de Leitenburg, G. Dolcetti, J.T. Kiss, J. Catal. 169 (1997) 490.
[16] N. Sergent, J.F. Lamonier, A. Aboukais, Chem. Mater. 12 (2000) 3830.
[17] G. Adachi, N. Imanaka, Chem. Rev. 98 (1998) 1479.
[18] S.H. Overbury, D.R. Huntley, D.R. Mullins, G.N. Glavee, Catal. Lett. 51 (1998) 133.
[19] D. Terrible, A. Trovarelli, J. Llorca, C. De Leitenburg, G. Dolcetti, J. Catal. 178 (1998) 299.
[20] M.F. Garcia, A.M. Arias, A.I. Jues, C. Belver, A.B. Hungrfa, J.C. Conesa, J. Soria, J. Catal. 194 (2000) 385.
[21] M. Hirano, E. Kato, J. Ceram. Soc. Jpn. 104 (1996) 958.
[22] T.V. Mani, H.K. Varma, A.D. Damodaran, K.G.K. Warrier, Ceram. Int. 19 (1993) 125.
[23] N. Izu, N. Murayama, W. Shin, I. Matsubara, S. Kanzaki, Jpn. J. Appl. Phys. 43 (2004) 6920.
[24] W. Bui, K.L. Choy, N.H.J. Stelzer, J. Scoonman, J. Solid State Ionics 116 (1999) 225.
[25] J. Kim, W. Myeong, S. Ihm, Appl. Catal. B 71 (1–2) (2007) 57–63.
[26] B.M. Reddy, G.K. Reddy, A. Khan, I. Ganesh, J. Mater. Sci. 42 (2007) 3557.
[27] B.M. Reddy, G.K. Reddy, I. Ganesh, J.M.F. Ferreira, J. Mater. Sci. 44 (2009) 2743.
[28] S. Bhaduri, S.B. Bhaduri, E. Zhou, J. Mater. Res. 13 (1998) 156.
[29] H.P. Klug, L.E. Alexander, X-ray Diffraction Procedures for Polycrystalline and Amorphous Materials, 2nd ed., Wiley, New York, 1974.
[30] B.M. Reddy, G.K. Reddy, K.N. Rao, A. Khan, I. Ganesh, J. Mol. Catal. A: Chem. 265 (2007) 276.
[31] B.M. Reddy, K.N. Rao, G.K. Reddy, A. Khan, S.E. Park, J. Phys. Chem. C 111 (2007) 18751.
[32] B.M. Reddy, I. Ganesh, A. Khan, J. Mol. Catal. A: Chem. 223 (2004) 295.
[33] B.M. Reddy, A. Khan, Y. Yamada, T. Kobayashi, S. Loridant, J.C. Volta, Langmuir 19 (2003) 3025.
[34] B.M. Reddy, P. Lakshmanan, S. Loridant, Y. Yamada, T. Kobayashi, C. Cartes, T.C. Rojas, A. Fernandez, J. Phys. Chem. B 110 (2006) 9140.
[35] B.M. Reddy, P. Lakshmanan, P. Bharali, P. Saikia, G. Thrimurthulu, M. Muhler, W. Gruenert, J. Phys. Chem. C 111 (2007) 10478.
[36] B.M. Reddy, P. Bharali, P. Saikia, A. Khan, S. Loridant, M. Muhler, W. Gruenert, J. Phys. Chem. C 111 (2007) 1878.
[37] J.R. McBride, K.C. Hass, B.D. Poindexter, W.H. Weber, J. Appl. Phys. 76 (1994) 2435.
[38] B.M. Reddy, A. Khan, Y. Yamada, T. Kobayashi, S. Loridant, J.C. Volta, J. Phys. Chem. B 106 (2002) 10964.
[39] W.H. Weber, K.C. Hass, J.R. McBride, Phys. Rev. B 48 (1993) 178.
[40] V.S. Escribano, E.F. Lopez, M. Panizza, C. Resini, J.M.G. Amores, G. Busca, Solid State Sci. 5 (2003) 1369.
[41] V. Solinas, E. Rombi, I. Ferino, M.G. Cutrufello, G. Colon, J.A. Navio, J. Mol. Catal. A: Chem. 204–205 (2003) 629.
[42] M.G. Cutrufello, I. Ferino, E. Rombi, V. Solinasa, G. Colón, J.A. Navio, React. Kinet. Catal. Lett. 79 (2003) 93.
[43] I. Ferino, M.F. Casula, A. Corrias, M.G. Cutrufello, R. Monaci, G. Paschina, Phys. Chem. Chem. Phys. 2 (2000) 1847.
[44] M.G. Cutrufello, I. Ferino, R. Monaci, E. Rombi, G. Colo, J.A. Nav, Phys. Chem. Chem. Phys. 3 (2001) 2928.
[45] S. Xu, X. Wang, Fuel 84 (2005) 563.
[46] H.S. Roh, H.S. Potdar, K.W. Jun, Catal. Today 93–95 (2004) 39.
[47] S. Larrondo, M.A. Vidal, B. Irigoyen, A.F. Craievich, D.G. Lamas, I.O. Fabregas, G.E. Lascalea, N.E. Walsoe de Reca, N. Amadeo, Catal. Today 107 (2005) 53.